Enhanced nutrient uptake is sufficient to drive emergent cross-feeding between bacteria in a synthetic community

Running title. Cross-feeding driven by enhanced nutrient uptake

Ryan K Fritts[1], Jordan T Bird[2], Megan G Behringer[3], Anna Lipzen[4], Joel Martin[4], Michael Lynch[3], and James B McKinlay[1]*

[1]Department of Biology, Indiana University Bloomington, Bloomington, IN, 47405

[2]Department of Biochemistry and Molecular Biology, University of Arkansas for Medical Sciences, Little Rock, AR, 72205

[3]School of Life Sciences, Biodesign Center for Mechanisms of Evolution, Arizona State University, Tempe, AZ, 85281

[4]Department of Energy Joint Genome Institute, Walnut Creek, CA, 94598

*Corresponding author

1001 E 3rd St, Jordan Hall, Bloomington, IN 47405

Phone: 812-855-0359

Email: jmckinla@indiana.edu

The authors declare no competing financial interests.

ABSTRACT

Interactive microbial communities are ubiquitous, influencing biogeochemical cycles and host health. One widespread interaction is nutrient exchange, or cross-feeding, wherein metabolites are transferred between microbes. Some cross-fed metabolites, such as vitamins, amino acids, and ammonium (NH_4^+), are communally valuable and impose a cost on the producer. The mechanisms that enforce cross-feeding of communally valuable metabolites are not fully understood. Previously we engineered mutualistic cross-feeding between N_2-fixing *Rhodopseudomonas palustris* and fermentative *Escherichia coli*. Engineered *R. palustris* excreted essential nitrogen as NH_4^+ to *E. coli* while *E. coli* excreted essential carbon as fermentation products to *R. palustris*. Here, we enriched for nascent cross-feeding in cocultures with wild-type *R. palustris*, not known to excrete NH_4^+. Emergent NH_4^+ cross-feeding was driven by adaptation of *E. coli* alone. A missense mutation in *E. coli* NtrC, a regulator of nitrogen scavenging, resulted in constitutive activation of an NH_4^+ transporter. This activity likely allowed *E. coli* to subsist on the small amount of leaked NH_4^+ and better reciprocate through elevated excretion of organic acids from a larger *E. coli* population. Our results indicate that enhanced nutrient uptake by recipients, rather than increased excretion by producers, is an underappreciated yet possibly prevalent mechanism by which cross-feeding can emerge.

INTRODUCTION

Microorganisms typically exist as members of diverse and interactive communities wherein nutrient exchange, also known as cross-feeding, is thought to be ubiquitous [1-7]. The prevalence of cross-feeding might explain, in part, why many microbes cannot synthesize essential vitamins and amino acids (i.e. auxotrophy), as they can often acquire these compounds from other community members [1, 7, 8]. Furthermore, microbes in nature experience varying degrees of starvation and often exist in states of low metabolic activity [9, 10]. Thus, cross-feeding might also serve to sustain microbes through starvation. Despite the

prevalence of cross-feeding, elucidating the molecular mechanisms underlying emergent cross-feeding interactions and tracking their evolutionary dynamics within natural microbial communities is difficult due to their sheer complexity. To overcome this intrinsic complexity, tractable synthetic consortia have proven useful for studying aspects of the mechanisms, ecology, evolution, and applications of microbial communities [4, 11-16].

To study the molecular mechanisms of nutrient cross-feeding, we previously developed a bacterial coculture in which *Escherichia coli* and *Rhodopseudomonas palustris* reciprocally exchange essential metabolites under anaerobic conditions (Fig.1A) [17-20]. In this coculture, *E. coli* ferments glucose, a carbon source that *R. palustris* cannot consume, and excretes ethanol and organic acids, namely acetate, lactate, succinate, and formate, as waste products. The organic acids, with the exception of formate, serve as the sole carbon sources for *R. palustris* (Fig. 1A). In return, *R. palustris* fixes dinitrogen gas (N_2) via the enzyme nitrogenase and excretes ammonium (NH_4^+), which is the sole nitrogen source for *E. coli* (Fig. 1A). Because both species depend on essential nutrients provided by their partner, this coculture functions as a synthetic obligate mutualism.

NH_4^+ cross-feeding from *R. palustris* to *E. coli* is thought to depend on the equilibrium between NH_3 and NH_4^+. The small proportion of NH_3 present in neutral pH environments is membrane permeable and can diffuse out of cells [21, 22]. Leaked NH_4^+ can be recaptured by AmtB transporters [21], which in the case of *R. palustris* helps privatize valuable NH_4^+ (Fig. 1B) [17, 18]. NH_4^+ leakage is also limited through the strict regulation of N_2 fixation, including by the transcriptional activator NifA, so that energetically expensive N_2 fixation is only performed when preferred nitrogen sources, such as NH_4^+, are limiting [23]. Previously, we identified two types of mutations that increase NH_4^+ excretion by *R. palustris* during N_2 fixation and support coculture growth with *E. coli* [17]: (i) deletion of *amtB*, which prevents recapture of leaked NH_3, or (ii) a 48-bp deletion within *nifA* (denoted as NifA*), which locks NifA into an active conformation [24] (Fig.

1B). In contrast, wildtype *R. palustris* does not readily support coculture growth with *E. coli* due to insufficient NH_4^+ excretion [17].

While mutualistic cross-feeding of communally valuable NH_4^+ between *E. coli* and *R. palustris* can be rationally engineered, we questioned whether such an interaction could arise spontaneously. Herein we experimentally evolved cocultures pairing WT *E. coli* with either WT *R. palustris* or an engineered NifA* mutant in serially-transferred batch cultures for ~150 generations. In both cocultures, a mutualism was established and growth rates improved over serial transfers, but growth and metabolic trends remained distinct. By pairing ancestral and evolved isolates of each species, we determined that adaptation by *E. coli* was solely responsible for establishing a mutualism with WT *R. palustris*. Whole-genome sequencing and subsequent genetic verification identified a missense mutation in the *E. coli* transcriptional activator for nitrogen scavenging, NtrC, that was sufficient to enforce mutualistic NH_4^+ cross-feeding with WT *R. palustris*. This mutation results in constitutive AmtB expression, presumably enhancing NH_4^+ uptake. Our results suggest that mutations that improve acquisition of communally valuable nutrients by recipients are favored to evolve and can promote the emergence of stable cross-feeding within synthetic consortia, and potentially within natural communities.

MATERIAL AND METHODS

Bacterial strains and growth conditions. All strains and plasmids are listed in Supplementary Table S1. All *E. coli* strains used in this study are derived from the type strain MG1655 [25], unless noted otherwise. The WT and NifA* *R. palustris* strains used in Fig. 1 were the type strain CGA009 [26] and CGA676, respectively. CGA676 carries a 48 bp deletion in *nifA* [24]. The *R. palustris* strains used in experimental coculture evolution and subsequent experiments were CGA4001 and CGA4003, which are derived from CGA009 and CGA676, respectively, with both carrying an additional Δ*hupS* mutation, preventing H_2 oxidation.

E. coli was grown in lysogeny broth (LB)-Miller (BD Difco) or on LB plates with 1.5% agar at 30 or 37°C with gentamicin (Gm; 5-15 µg/ml), kanamycin (Km; 30 µg/ml), or carbenicillin (Cb; 100 µg/ml) when appropriate. *R. palustris* was grown in defined minimal photosynthetic medium (PM) [26] or on PM agar with 10 mM succinate at 30°C with Gm (100 µg/ml) when appropriate. N_2-fixing medium (NFM) was made by omitting $(NH_4)_2SO_4$ from PM. NFM and LB agar were used as selective media to quantify *R. palustris* and *E. coli* colony-forming units (CFUs), respectively. Experimental mono- and cocultures were grown in 10 ml of M9-derived coculture medium (MDC) in 27 ml anaerobic glass test tubes. Tubes were made anaerobic under 100% N_2, sterilized, and supplemented with 1 mM $MgSO_4$ and 0.1 mM $CaCl_2$ as described [17]. *E. coli* starter monocultures had 25 mM glucose and were growth-limited by supplementing with 1.5 mM NH_4Cl. *R. palustris* starter monocultures were growth-limited by supplementing with 3 mM acetate. Cocultures were inoculated by subculturing 1% v/v of starter monocultures of each species into MDC with 50 mM glucose. Mono- and cocultures were grown at 30 °C, under shaken conditions, lying horizontally and shaken at 150 rpm beneath a 60 W incandescent bulb (750 lumens), or under static conditions, standing vertically without shaking beside a 60 W incandescent bulb.

***E. coli* strain construction.** All primers are listed in Supplementary Table S2. To construct the *E. coli* $NtrC^{S163R}$ mutant, the Gm^R-*sacB* genes from pJQ200SK [27] were PCR amplified using primers containing ~40 bp overhangs with homology up- and downstream of *ntrC* (*glnG*). A second round of PCR was subsequently performed to increase the length of overhanging regions of homology to ~80 bp to increase the recombination frequency. *E. coli* harboring pKD46, encoding arabinose-inducible λ-red recombineering genes [28], was grown in LB with 20 mM arabinose and Cb at 30 °C to an OD_{600} of ~0.5 and then centrifuged, washed, and resuspended in sterile distilled water at ambient temperature. Resuspended cells were electroporated with the Gm^R-*sacB* PCR product containing overhangs flanking *ntrC* and plated on LB Gm agar. Gm-resistant colonies were screened by PCR for site-directed recombination of

125 Gm^R-*sacB* into the *ntrC* locus, creating a Δ*ntrC*::Gm^R-*sacB* allele, which was then verified by
126 sequencing. To replace the Δ*ntrC*::Gm^R-*sacB* locus, the $NtrC^{S163R}$ allele was PCR-amplified
127 from gDNA from evolved *E. coli* (lineage A25) and electroporated into *E. coli* Δ*ntrC*::Gm^R-*sacB*
128 harboring pKD46. After counterselection on LB agar with 10% (w/v) sucrose but without NaCl,
129 site-directed recombination of the $NtrC^{S163R}$ allele into the native locus was confirmed by PCR
130 and sequencing. *E. coli* $NtrC^{S163R}$ was grown overnight on LB agar at 42°C to cure the strain of
131 pKD46, which was confirmed by Cb sensitivity.
132 ***R. palustris* strain construction**. To construct *R. palustris* CGA4001 and CGA4003, pJQ-
133 Δ*hupS* was introduced into *R. palustris* CGA009 and CGA676, respectively, by conjugation with
134 *E. coli* S17-1. Mutants were then obtained using sequential selection and screening as
135 described [29]. The Δ*hupS* deletion was confirmed by PCR and sequencing.
136 **Analytical procedures.** Cell densities were approximated by optical density at 660 nm (OD_{660})
137 using a Genesys 20 visible spectrophotometer (Thermo-Fisher). Coculture doubling times were
138 derived from specific growth rates determined by fitting exponential functions to OD_{660}
139 measurements between 0.1-1.0 for each biological replicate. NH_4^+ was quantified using an
140 indophenol colorimetric assay [17]. Glucose and soluble fermentation products were quantified
141 by high-performance liquid chromatography (Shimadzu) as described [30]. H_2 was quantified by
142 gas chromatography (Shimadzu) as described [31].
143 **Coculture evolution experiments.** Founder monocultures of *E. coli* MG1655, *R. palustris*
144 CGA4001 (Δ*hupS*), and CGA4003 (Δ*hupS* NifA*) were inoculated from single colonies in MDC.
145 Once grown, a single founder monoculture of each strain was used to inoculate twelve WT-
146 based cocultures (six shaken: A-F; six static: G-L) and 12 NifA*-based cocultures (six shaken:
147 M-R; six static: S-X) in MDC with 50 mM glucose. Cocultures were serially transferred by
148 passaging 2% v/v of stationary phase coculture (OD_{660} > 2 and a low metabolic rate based on
149 H_2 measurements) into fresh MDC. The NifA*-based cocultures were transferred weekly
150 whereas WT-based cocultures were transferred every 21-50 days for the first five transfers and

then every two-weeks based on the time required to reach OD_{660} > 2. For comparative analyses, shaken cocultures (A-F and M-R) were revived from frozen stocks made following transfer-2 (generation 17) and transfer-25 (generation 146). Frozen stock (~0.2 ml) was thawed in 1 ml sterile MDC, washed 2X with MDC to remove glycerol, and then resuspended in 0.2 ml MDC for use as inoculum.

RNA extraction and reverse transcription quantitative PCR. RNA was isolated from exponentially growing *E. coli* monocultures or starved cell suspensions that had been chilled on ice, centrifuged at 4°C, cell pellets frozen using dry-ice in ethanol, and stored at -80°C. Cell pellets were thawed on ice, disrupted by bead beating, and then RNA was purified using an RNeasy MiniKit (Qiagen), Turbo DNase (Ambion) treatment on columns, and RNeasy MinElute Cleanup Kit (Qiagen). cDNA was synthesized from 0.5-1 µg of RNA per sample using Protoscript II RT and Random Primer Mix (New England Biolabs). qPCR reactions were performed on cDNA using iQ SYBR Green supermix (BioRad). *E. coli* gDNA was used to generate standard curves for *amtB* and *ntrC* transcript quantification, which were normalized to transcript levels of reference genes *gyrB* and *hcaT* [32]. Two technical replicate qPCR reactions were performed and averaged for each biological replicate to calculate relative expression.

Genome sequencing and mutation analysis. gDNA was extracted from stationary phase evolved cocultures following revival from frozen stocks using a Wizard Genomic DNA purification Kit (Promega). DNA fragment libraries were constructed for samples from shaking WT-based cocultures A-F and NifA*-based cocultures M-R at generation ~146 using NextFlex Bioo Rapid DNA kit. Samples were sequenced on an Illumina NextSeq 500 150 bp paired-end run by the Indiana University Center for Genomics and Bioinformatics. Paired-end reads were trimmed using Trimmomatic 0.36 [33] with the following options: LEADING:3 TRAILING:3 SLIDINGWINDOW:10:26 HEADCROP:10 MINLEN:36. Mutations were called using *breseq* version 0.32.0 on Polymorphism Mode [34] and compared to a reference genome created by concatenating *E. coli* MG1655 (Accession NC_000913), *R. palustris* CGA009 (Accession

177 BX571963), and its plasmid pRPA (Accession BX571964). Mutations are summarized in
178 Supplemental File 1.
179 Additional gDNA sequencing for evolved WT-based cocultures A-F (shaking, generation 11), G-
180 L (static, generations 11 and 123), and NifA*-based cocultures S-X (static, generation 123) was
181 performed at the US Department of Energy Joint Genome Institute. Plate-based DNA library
182 preparation for Illumina sequencing was performed on the PerkinElmer Sciclone NGS robotic
183 liquid handling system using Kapa Biosystems library preparation kit. 200 ng of gDNA was
184 sheared using a Covaris LE220 focused-ultrasonicator. Sheared DNA fragments were size
185 selected by double-SPRI and selected fragments were end-repaired, A-tailed, and ligated with
186 Illumina compatible sequencing adaptors from IDT containing a unique molecular index barcode
187 for each sample library. Libraries were quantified using KAPA Biosystem's next-generation
188 sequencing library qPCR kit and run on a Roche LightCycler 480 real-time PCR instrument. The
189 quantified libraries were then prepared for sequencing on the Illumina HiSeq sequencing
190 platform utilizing a TruSeq Rapid paired-end cluster kit. Sequencing was performed on the
191 Illumina HiSeq2500 sequencer using HiSeq TruSeq SBS sequencing kits, following a 2x100
192 indexed run recipe. Reads were aligned to a reference genome created by concatenating *E. coli*
193 MG1655 (Accession NC_000913), *R. palustris* CGA009 (Accession NC_005296), and its
194 plasmid pRPA (Accession NC_005297) [35]. The resulting bams were then split by organism
195 and down sampled to 100 fold depth if in excess of that, then re-merged to create a normalized
196 bam for calling single nucleotide polymorphisms and small indels by callVariants.sh from the
197 BBMap package (sourceforge.net/projects/bbmap/) to capture variants present within the
198 population and annotation applied with snpEff [36]. Mutations are summarized in Supplemental
199 File 2.
200 All FASTQ files are available at NCBI Sequence Read Archive (Accession numbers listed in
201 Supplementary Table S3)
202

RESULTS

Nascent emergence of mutualistic cross-feeding between wild-type *R. palustris* and *E. coli*. Previously, we engineered *R. palustris* to excrete NH_4^+ (NifA*) to stabilize mutualistic cross-feeding with *E. coli* (Fig. 1A and B). Here, we sought to determine whether such a relationship could evolve spontaneously. Spatial proximity has been shown to be an important factor in many microbial cross-feeding mutualisms [37, 38], which can be disrupted by mixing. To account for the possible importance of proximity, we established cocultures with WT *R. palustris* (WT-based cocultures) under both shaken conditions, wherein cells are evenly distributed, and static conditions, wherein cells settle in close proximity at the bottom of the tube. In parallel, we also established shaken and static cocultures featuring the *R. palustris* NifA* strain (NifA*-based cocultures) as a comparative reference.

We confirmed our previous observations [17] that WT *R. palustris* exhibits undetectable NH_4^+ excretion and does not readily support coculture growth with WT *E. coli*, in contrast to the NifA* mutant (Fig. 1C and D). Whereas shaken NifA*-based cocultures grew to an OD_{660} > 2.0 in 4-6 days with a doubling time of ~12 h, shaken WT-based cocultures did not exhibit appreciable growth in the same time frame (Fig. 1D). We hypothesized that prolonged incubation might enrich for spontaneous mutants that permit coculture growth. Indeed, after 50 days, shaken WT-based cocultures reached densities similar to those observed for NifA*-based cocultures, albeit with a doubling time of ~13 days (Fig. 1D). Static WT- and NifA*-based cocultures also became turbid within this time frame.

Upon observing a nascent mutualism between WT *R. palustris* and *E. coli*, we set up new cocultures to experimentally evolve six replicates of WT-based cocultures (A-F) and NifA*-based cocultures (M-R) through serial transfers under shaken conditions, all with WT *E. coli* (Fig. 2A), to compare their physiology, evolutionary trajectory, and species and genotypic composition. We also serially transferred static WT-based cocultures (G-L) and NifA*-based cocultures (S-X). However, we herein focus the bulk of our analyses on shaken cocultures

because (i) the close proximity provided under static conditions was not required for nascent cross-feeding, (ii) shaken conditions facilitate analyses such as OD-based determination of growth rates, and (iii) strong biofilms emerged in static cocultures, complicating the determination of population densities.

Shaken WT- and NifA*-based cocultures were serially transferred 25 times, corresponding to ~146 generations, with ~5.6 generations estimated per serial coculture (including the original cocultures designated, transfer-0) based on the 1:50 dilution used for each transfer. This number of generations corresponded to ~ 65 weeks for WT-based cocultures and ~ 26 weeks for NifA*-based cocultures. We then revived cocultures from frozen stocks at transfer-2 (generation 17; G17) and transfer-25 (generation 146; G146) time point to compare growth and population trends. At G17, NifA*-based cocultures exceeded an OD_{660} of 2 in under 8 days whereas WT-based cocultures took ~40 days (Fig. 2B). By G146, the time needed to reach $OD_{660} > 2$ had decreased for every lineage (Fig. 2C). The shortened growth phase was most pronounced for WT-based cocultures, which all reached $OD_{660} > 2$ in under 17 days by G146, less than half the time needed at G17 (Fig. 2B, C); WT-based coculture doubling times decreased from 135 ± 55 h to 47 ± 10 h (Fig. 2D). Though less drastic, NifA*-based coculture doubling times also decreased, in this case from ~11 h to ~8 h (Fig. 2D). Thus, WT-based cocultures adapted to grow faster, although never as fast as unevolved engineered NifA*-based cocultures.

Because growth trends differed between WT- and NifA*-based cocultures, we wondered how species populations were affected. We therefore enumerated viable cells as colony forming units (CFUs) at the final time points for G17 and G146 cocultures shown in Fig. 2A and B. At G17, both *R. palustris* and *E. coli* populations in WT-based cocultures were lower than those in NifA*-based cocultures (Fig. 3A). It is worth noting that NifA*-based cocultures were plated after ~10 days, whereas WT-based cocultures were plated after 39-43 days due to their slower growth rate. Consequently, the background death rate during the additional ~30 days of slower

255 growth for WT-based cocultures could have contributed to the lower final CFUs. At G146, *R.*
256 *palustris* abundances in WT-based cocultures had increased >14-fold and exceeded *R.*
257 *palustris* abundances observed in NifA*-based cocultures by ~2-fold (Fig. 3). *E. coli* abundances
258 in WT-based cocultures also increased >7-fold by G146, but did not reach abundances
259 observed in NifA*-based cocultures (Fig. 3). The increase in *E. coli* abundances in WT-based
260 cocultures by G146 suggests that *E. coli* had better access to NH_4^+, or other nitrogen
261 compounds than at G17 (Fig. 3B). Due to the disproportionate increase in each population in
262 WT-based cocultures between G17 and G146, *E. coli* percentages remained low at 1-5%,
263 relative to 11-21% in NifA*-based cocultures (Fig. 3B). These differences in *E. coli* populations
264 between WT- and NifA*-based cocultures are consistent with previous findings that higher NH_4^+
265 excretion by *R. palustris* supports faster growth and higher *E. coli* abundances [17-19].
266 In contrast to WT-based cocultures, NifA*-based cocultures did not display drastically
267 higher cell densities for each species between G17 and G146 (Fig. 3). Average *E. coli* densities
268 were 4.7 x 10^8 CFUs/ml and 6.9 x 10^8 CFUs/ml at G17 and G146, respectively. Average *R.*
269 *palustris* densities were 3.4 x 10^9 CFUs/ml and 3.9 x 10^9 CFUs/ml at G17 and G146,
270 respectively. The average *E. coli* percentage in NifA*-based cocultures was similar at G17
271 (16.5%) and at G146 (16.4%) (Wilcoxon matched-pairs signed rank test, P=0.563).
272
273 **Metabolic differences between WT- and NifA*-based cocultures help explain growth and**
274 **population trends.** Our studies demonstrated that growth and population trends in coculture
275 are strongly influenced by cross-feeding levels of both NH_4^+ and organic acids [17-19]. For
276 instance, higher NH_4^+ cross-feeding to *E. coli* leads to higher *E. coli* growth rates [17-19]. In
277 turn, higher *E. coli* growth rates boost organic acid excretion, supporting better *R. palustris*
278 growth up until the organic acid excretion rate exceeds the rate at which *R. palustris* can
279 consume them [17]. To see if such trends were also present in WT-based cocultures, we
280 quantified glucose consumption and fermentation product yields at G17 and G146 at stationary

phase. At G17, glucose consumption by *E. coli* in WT-based cocultures was about half of that in NifA*-based cocultures (Fig. 4A). The lower glucose consumption in WT-based cocultures can explain in part the lower *E. coli* CFUs observed in Fig. 3A. Previously, we showed that non-growing *E. coli* can ferment glucose, and that this growth-independent fermentation can provide sufficient carbon to support *R. palustris* growth [19]. We hypothesize that growth-independent fermentation by *E. coli* was an important cross-feeding mechanism during the extremely slow growth of early WT-based cocultures (Fig. 1D). However, by G146, *E. coli* glucose consumption in WT-based cocultures approached that in NifA*-based cocultures in most lineages, with one lineage consuming more glucose than NifA*-based cocultures (Fig. 4A). The general increase in *E. coli* glucose consumption in WT-based cocultures from G17 to G146 likely supported both the faster coculture doubling times (Fig. 2D) and higher *E. coli* abundances (Fig. 3B) and contributed to the accumulation of consumable organic acids such as acetate and succinate in some WT-based cocultures at G146, qualitatively similar to NifA*-based cocultures (Fig. S2). Overall, the increase in metabolic activities attributed to *E. coli* and the improved *E. coli* growth in WT-based cocultures between G17 and G146 suggests that nitrogen cross-feeding also increased.

We observed a potential trade-off between coculture growth rate and coculture growth yield (ΔOD_{660}/glucose consumed). For example, WT-based G17 cocultures had the slowest growth rates but highest growth yields, whereas NifA*-based G146 cocultures had the fastest growth rates but lowest growth yields (Fig. 4B). Trade-offs between growth rate and yield have been reported in multiple microbial species under various conditions [39-41]. In our case, the metabolic trends point to possible explanations for the apparent trade-off. For example, formate produced by *E. coli* is not consumed by *R. palustris* and thus typically accumulates in cocultures [17]. However, no formate was detected in WT-based G17 cocultures and formate yields were approximately half that of NifA*-based cocultures at G146 (Fig. 4C). Low formate yields could be explained in part by increased conversion of formate to H_2 and CO_2 by *E. coli* formate

hydrogenlyase [42, 43]. Consistent with this possibility, WT-based cocultures had the highest H_2 yields (Fig. 4D). Low formate yields could also be explained by decreased formate production by *E. coli* in favor of other fermentation products. We previously observed low formate yields in slow-growing, nitrogen-limited NifA*-based cocultures [19, 20], suggesting that formate production by *E. coli* varies in response to growth rate. We have also not ruled out the possibility that *R. palustris* can consume some formate under certain conditions. In addition to formate, consumable organic acid yields were also lower at both G17 and G146 for WT-based cocultures relative to NifA*-based cocultures (Fig. S2). Organic acid accumulation in cocultures can acidify the medium to inhibitory levels [17] . At both G17 and G146, the lower yields of formate and other organic acids in WT-based cocultures translated into higher pH values than in NifA*-based cocultures (Fig. 4E). This lower level of acidification combined with the likelihood of a higher proportion of glucose being fermented into organic acids other than formate could explain the higher *R. palustris* cell densities at G146 in WT-based cocultures compared to NifA*-based cocultures (Fig. 3B).

A single mutation in an *E. coli* nitrogen starvation response regulator is sufficient for mutualistic growth with WT *R. palustris*. We hypothesized that the growth of WT-based cocultures was due to adaptive mutations in one or both species. To determine whether the evolution of either or both species was necessary to establish a nascent mutualism, we isolated single colonies of each species from ancestral WT populations and evolved G146 cocultures and paired them in all possible combinations (Fig. 5A). Only those pairings featuring evolved *E. coli* grew to an OD_{660} >0.5 after ~24 days (Fig. 5B). Cocultures pairing evolved *E. coli* with ancestral or evolved WT *R. palustris* exhibited similar doubling times of ~67 h (Fig. S1). These results indicate that adaptation by *E. coli* alone is sufficient to establish a nascent mutualism with WT *R. palustris*. Accordingly, we did not observe increased NH_4^+ excretion in evolved WT *R. palustris* N_2-fixing monocultures compared to the ancestral strain (Fig. S1).

To identify candidate mutations in *E. coli* that could drive improved coculture growth, we sequenced the genomes of populations in each evolved coculture lineage after 123-146 generations. We also sequenced WT-based cocultures following ~11 generations to determine if potentially adaptive mutations arose early within WT-based cocultures. Several parallel mutations were identified in both species at frequencies between 5 and 100% (Table 1 and Supplementary Files 1 and 2). Consistent with evolved *E. coli* being necessary for mutualistic growth with either ancestral or evolved WT *R. palustris* (Fig. 5B), we did not detect any *nifA* nor *amtB* mutations in evolved WT *R. palustris* populations, which would enable rapid coculture growth. The multiple high frequency parallel mutations observed in evolved *R. palustris* populations (Table 1), are insufficient to improve coculture growth trends (Fig. 5B). Of the mutations in evolved *E. coli* populations, we were intrigued by a fixed missense mutation in *glnG* (henceforth called *ntrC*) that occurred in all evolved *E. coli* populations from both shaken and static WT-based cocultures, replacing serine 163 with an arginine within the AAA+ domain in the encoded the response regulator NtrC ($NtrC^{S163R}$, Table 1 and Fig. 5C). NtrC and the histidine kinase NtrB form a two-component system that senses and coordinates the nitrogen starvation response in *E. coli* [44-46]. Our lab previously found that the *E. coli* NtrBC-regulon is highly expressed in coculture with *R. palustris* NifA* [20]. Thus, *E. coli* NtrBC might be even more important in coculture with WT *R. palustris* wherein *E. coli* nitrogen starvation is expected to be intensified.

The $NtrC^{S163R}$ mutation was enriched early in the evolution of WT-based cocultures, already at a high frequency in most lineages by G11 (Table 1 and Supplementary Table 3). Because of the striking parallelism of the $NtrC^{S163R}$ mutation across coculture lineages, we wondered if it was present as standing genetic variation in the ancestral *E. coli* population. We therefore sequenced *ntrC* of ten *E. coli* isolates subjected to a single round (35 days) of coculture growth with WT *R. palustris* (Fig. 6A), which should enrich for the $NtrC^{S163R}$ mutation. All ten isolates sequenced had the WT *ntrC* allele. Thus, although the $NtrC^{S163R}$ allele was likely

present in the founder population given its presence in every WT-based coculture lineage, it was likely under strong selection from an initial low frequency. In support of the importance of the NtrC^{S163R} allele, we also identified multiple, though different, high frequency mutations in *ntrB* and *ntrC* in *E. coli* populations from NifA*-based cocultures evolved under both well-mixed and static conditions (Table 1 and Supplementary Table 3). Together, these observations strongly suggest the adaptive importance of *E. coli ntrBC* mutations like NtrC^{S163R} for coculture growth, regardless of the NH_4^+-excreting phenotype of the *R. palustris* partner.

To determine if the NtrC^{S163R} mutation alone was sufficient to support coculture growth with WT *R. palustris,* we moved the NtrC^{S163R} allele into the ancestral *E. coli* strain. Cocultures pairing *E. coli* NtrC^{S163R} with WT *R. palustris* grew with a doubling time of 124 ± 22 h, approximately twice as long as cocultures with evolved *E. coli* isolates, but much faster than cocultures with ancestral *E. coli* (Fig. 6A). Thus, the NtrC^{S163R} mutation is sufficient to drive coculture growth. Cocultures with *E. coli* NtrC^{S163R} reached similar final cell densities, but supported lower WT *R. palustris* abundances than cocultures with evolved *E. coli* isolates (Fig. 6B).

We speculate that some of the additional parallel mutations in evolved *E. coli* (Table 1) are also adaptive and account for the faster coculture growth rate relative to cocultures with the NtrC^{S163R} mutant (Fig. 6A). For example, the *E. coli* strain we used has a frameshift mutation in *rph* that decreases expression of *pyrE* immediately downstream [47]. Mutations in *rph* and in-between *rph* and *pyrE*, like those identified here (Table 1 and Supplementary Files 1 and 2), can improve pyrimidine biosynthesis and growth in minimal media [48]. HdfR is a transcriptional regulator that inhibits flagellar expression [49] and activates glutamate synthase expression [50]. HdfR loss-of-function mutations could reduce glutamate synthase expression and synchronize NH_4^+ assimilation with the low NH_4^+ cross-feeding levels in WT-based cocultures. However, the entire HdfR regulon has never been reported and thus could include other genes. In another possible link to nitrogen metabolism, mutations accumulated in the glutamine tRNA

gene, *glnX* (Table 1). Two of the mutations disrupt the base-pair adjacent to the anti-codon loop while two others alter the anti-codon, one still coding for glutamine but the other coding for histidine. The impact of these mutations is difficult to predict, especially since GlnX is just one of four *E. coli* tRNAs for glutamine. The *yhdWXYZ* operon encodes an NtrC-regulated amino acid ABC transporter, which is predicted to be non-functional due to a frameshift mutation in *yhdW* [44, 45]. The mutations identified in (Table 1) and directly upstream of the *yhdW* pseudogene (Supplementary Files 1 and 2) could restore amino acid transport for use as a nitrogen source or alternatively disrupt NtrC binding upstream of *yhdW* and thereby free up NtrC to regulate genes more critical to NH_4^+ acquisition.

The *E. coli* NtrC^{S163R} allele constitutively activates ammonium transporter expression. Based on the effects of NtrC mutations observed by others [51, 52], we hypothesized that the NtrC^{S163R} allele facilitates coculture growth with WT *R. palustris* by conferring constitutive expression of NtrBC-regulated genes important for NH_4^+ acquisition. We previously determined that NtrC and AmtB were crucial gene products within the NtrBC regulon for growth and coexistence with *R. palustris* NifA* [18, 20]. To test if the NtrC^{S163R} allele increased *amtB* and *ntrC* expression, we measured transcript levels by reverse transcription quantitative PCR (RT-qPCR) in *E. coli* monocultures grown with 15 mM NH_4Cl or subjected to complete nitrogen starvation (~10 h with 0 mM NH_4Cl). We chose to perform RT-qPCR on *E. coli* monocultures, because ancestral WT *E. coli* does not readily grow with WT *R. palustris* and because *E. coli* typically constitutes a low percentage (1-5%) of WT-based cocultures, meaning most mRNA would be from *R. palustris*.

When cultured with NH_4Cl, the *E. coli* NtrC^{S163R} mutant exhibited ~30 and ~15-fold higher expression of *amtB* and *ntrC*, respectively, than WT *E. coli* (Fig. 6C), indicating that the NtrC^{S163R} allele constitutively activates expression of its regulon. Following 10 h of nitrogen

starvation, we saw similarly high *amtB* and *ntrC* expression by both the WT and the NtrC^{S163R} strains (Fig. 6C). Thus, both the WT and NtrC^{S163R} *E. coli* strains are able to commence strong transcriptional responses to extreme nitrogen starvation. We expect that the level of nitrogen limitation experienced by *E. coli* in coculture with WT *R. palustris* is less extreme than the complete nitrogen starvation conditions used in our qPCR experiments. Although we cannot detect NH_4^+ excretion by WT *R. palustris*, the equilibrium with NH_3 dictates that some will be excreted, possibly within the nM to low µM range where AmtB is critical [21]. We also know that AmtB is important in coculture for *E. coli* to compete for transiently available NH_4^+ that *R. palustris* will otherwise reacquire [18]. We therefore hypothesize that the NtrC^{S163R} mutation primes *E. coli* for coculture growth with *R. palustris* by maintaining high AmtB expression and thereby enabling acquisition of scarcely available NH_4^+. The resulting faster *E. coli* growth and metabolism would translate into faster organic acid excretion, which itself would foster *R. palustris* growth and reciprocal NH_4^+ excretion. Thus, we envision that better NH_4^+ acquisition creates a positive feedback loop, enhancing the growth of both players in the mutualism.

DISCUSSION

Here, we determined that in cocultures requiring nitrogen transfer from *R. palustris to E. coli*, an *E. coli* NtrC^{S163R} mutation alone is sufficient to enable coculture growth. The mutation results in constitutive activity of the NtrC regulon and thus increased expression of the AmtB NH_4^+ transporter, which we hypothesize enhances NH_4^+ uptake. This is the first mutation we have identified in the NH_4^+ recipient *E. coli* that is sufficient to support mutualistic growth with WT *R. palustris*. Overall, our data suggest that a recipient species can persuade cross-feeding through enhanced nutrient uptake. An improvement in nutrient acquisition by one species could lead to increased reciprocation and thus generate a positive feedback loop in the context of mutualism.

Our previous work on this consortium utilized *R. palustris* NifA* and ΔAmtB strains that we engineered to excrete NH_4^+ [17-19]. In the present study, we did not identify *nifA* or *amtB*

436 mutations in evolved WT *R. palustris* populations. *R. palustris nifA* and *amtB* mutations likely
437 incur a fitness cost, such as an increased energetic burden of constitutive nitrogenase
438 expression due to the NifA* mutation or loss of NH_4^+ to WT competitors in the case of an
439 inactivating *amtB* mutation. Thus, emergent *R. palustris nifA* and *amtB* mutants would not be
440 expected to be competitive in the presence of a large WT *R. palustris* population. However, it
441 does not appear that *R. palustris* NifA* regained regulation of nitrogenase and limited NH_4^+
442 excretion during the experimental evolution of NifA*-based cocultures. Instead, ancestral and
443 evolved NifA*-based cocultures supported consistent abundances of *E. coli*, a trait that is
444 dependent on the level of NH_4^+ excretion [17-19]. Our results therefore suggest that the NifA*
445 mutation, a 48-bp deletion, is not prone to frequent or rapid suppression, at least during the time
446 scale of this study, potentially because multiple mutations would be required. It is also possible
447 that the cost of constitutive N_2 fixation is relatively low within this mutualism. Based on our
448 findings, we propose that experimental evolution of synthetic consortia is useful for both for
449 identifying novel genotypes enabling coexistence and for assessing the stability of putatively
450 costly engineered genotypes.

451 More broadly, our results indicate that within a cross-feeding partnership, multiple
452 combinations of recipient and producer genotypes can lead to stable coexistence but only
453 certain combinations will be favored based on the selective environment. Under well-mixed
454 conditions there is intense competition between recipients as well as producers for limiting,
455 communally-valuable nutrients, such as NH_4^+ [18], vitamins, or amino acids [1, 7, 8].
456 Additionally, there is a probable fitness cost for producers associated with increased nutrient
457 excretion in well-mixed environments. Under well-mixed conditions, costless self-serving and
458 mutually beneficial mutations, but not costly partner-serving mutations, are favored to evolve
459 [53]. Therefore mutations that improve a recipient's ability to acquire nutrients from producers,
460 and thereby outcompete other recipient genotypes, can evolve rapidly [54]. Recipient mutations
461 that enhance metabolite uptake also erode the partial privatization of communally valuable

462 nutrients released by the producer [55]. Even so, these recipient mutations can benefit
463 producers if they promote mutualistic interactions [54]. We view the *E. coli* NtrC^{S163R} mutation as
464 an example of a conditionally-costless self-serving mutation, given its rapid emergence in well-
465 mixed cocultures, but one that is mutually beneficial in the context of an obligate mutualism. We
466 hypothesize that the benefit of the NtrC^{S163R} mutation for *E. coli* extends more generally to
467 surviving nitrogen limitation. In support of this, an NtrC^{V18L} mutation that similarly increased
468 *amtB* expression was adaptive for *E. coli* evolved in nitrogen-limiting monocultures [56]. *E. coli*
469 is nitrogen-limited in all coculture conditions used in this study, likely explaining why *E. coli*
470 NtrBC mutations were also observed in evolved NifA*-based cocultures, and in all static
471 cocultures, where the dense populations at the bottom of the test tube likely intensify
472 competition for NH_4^+.

473 Mutations that improve nutrient acquisition can be mutually beneficial for cross-feeding
474 partners under conditions where neither species can grow well without reciprocal nutrient
475 exchange. However, mutations that enhance nutrient uptake could also be adaptive for the
476 recipient when there is no reciprocal benefit to the producer. For example, acetate cross-feeding
477 repeatedly evolved in *E. coli* populations under glucose-limiting conditions through mutations
478 that enhanced acetate uptake by a nascent recipient subpopulation [57, 58]. Unlike in our study,
479 the acetate-consuming recipients did not provide a clear reciprocal benefit to the acetate-
480 excreting producers beyond a potentially relaxed competition for glucose due to resource
481 partitioning [57, 58]. Consequently, mutations that enhance nutrient uptake could foster the
482 emergence of mutualistic, commensal, or competitive interactions, depending on community
483 composition and conditions [54, 57, 58]. In natural microbial communities, where auxotrophy is
484 prevalent [1, 7] and most cells exhibit low metabolic activity [9, 10], mutations that improve
485 acquisition of limiting nutrients could allow certain populations to flourish. Understanding the
486 consequences of mutations that expedite metabolite acquisition could thus inform on the origins
487 of various ecological relationships. This knowledge could ultimately be harnessed for

488 applications ranging from facilitating coexistence within synthetic consortia to probiotic-mediated
489 competitive exclusion of pathogens.
490
491 **Acknowledgements**
492 This work was supported in part by U.S. Army Research Office grants W911NF-14-1-0411 and
493 W911NF-17-1-0159, a National Science Foundation CAREER award MCB-1749489, the U.S.
494 Department of Energy, Office of Science, Office of Biological and Environmental Research,
495 under award DE-SC0008131, and the Joint Genome Institute Community Science Program,
496 CSP 502893. The work conducted by the U.S. Department of Energy Joint Genome Institute, a
497 DOE Office of Science User Facility, is supported by the Office of Science of the U.S.
498 Department of Energy under Contract No. DE-AC02-05CH11231.
499 We thank AL Posto, JR Gliessman, and MC Onyeziri for coculture passaging and initial
500 characterizations, JT Lennon and BK Lehmkuhl for equipment and assistance with qRT-PCR,
501 and J Ford and AM Buechlein at the IU Center for Genomics and Bioinformatics.
502
503 **References**
504 1. Seth EC, Taga ME. Nutrient cross-feeding in the microbial world. Front Microbiol.
505 2014;5:350.
506 2. Estrela S, Trisos CH, Brown SP, Associate Editor: Pejman R, Editor: Troy D. From
507 Metabolism to Ecology: Cross-Feeding Interactions Shape the Balance between Polymicrobial
508 Conflict and Mutualism. Am Nat. 2012;180:566-76.
509 3. Morris BEL, Henneberger R, Huber H, Moissl-Eichinger C. Microbial syntrophy:
510 interaction for the common good. FEMS Microbiol Rev. 2013;37:384-406.
511 4. Ponomarova O, Patil KR. Metabolic interactions in microbial communities: untangling the
512 Gordian knot. Curr Opin Microbiol. 2015;27:37-44.
513 5. Zelezniak A, Andrejev S, Ponomarova O, Mende DR, Bork P, Patil KR. Metabolic
514 dependencies drive species co-occurrence in diverse microbial communities. Proc Natl Acad
515 Sci USA. 2015;112:6449-54.
516 6. Embree M, Liu JK, Al-Bassam MM, Zengler K. Networks of energetic and metabolic
517 interactions define dynamics in microbial communities. Proc Natl Acad Sci USA.
518 2015;112:15450-5.
519 7. Zengler K, Zaramela LS. The social network of microorganisms — how auxotrophies
520 shape complex communities. Nat Rev Microbiol. 2018;16:383-90.
521 8. Mee MT, Collins JJ, Church GM, Wang HH. Syntrophic exchange in synthetic microbial
522 communities. Proc Natl Acad Sci USA. 2014;111:E2149-E56.

9. Bergkessel M, Basta DW, Newman DK. The physiology of growth arrest: uniting molecular and environmental microbiology. Nat Rev Microbiol. 2016;14:549-62.
10. Lennon JT, Jones SE. Microbial seed banks: the ecological and evolutionary implications of dormancy. Nat Rev Microbiol. 2011;9:119-30.
11. Momeni B, Chen C-C, Hillesland KL, Waite A, Shou W. Using artificial systems to explore the ecology and evolution of symbioses. Cell Mol Life Sci. 2011;68:1353-68.
12. Mee MT, Wang HH. Engineering ecosystems and synthetic ecologies. Mol Biosyst. 2012;8:2470-83.
13. Lindemann SR, Bernstein HC, Song H-S, Fredrickson JK, Fields MW, Shou W, et al. Engineering microbial consortia for controllable outputs. ISME J. 2016;10:2077-84.
14. Widder S, Allen RJ, Pfeiffer T, Curtis TP, Wiuf C, Sloan WT, et al. Challenges in microbial ecology: building predictive understanding of community function and dynamics. ISME J. 2016;10:2557-68.
15. Hillesland KL, Stahl DA. Rapid evolution of stability and productivity at the origin of a microbial mutualism. Proc Natl Acad Sci USA. 2010;107:2124-9.
16. Harcombe WR, Riehl WJ, Dukovski I, Granger BR, Betts A, Lang AH, et al. Metabolic resource allocation in individual microbes determines ecosystem interactions and spatial dynamics. Cell Rep. 2014;7:1104-15.
17. LaSarre B, McCully AL, Lennon JT, McKinlay JB. Microbial mutualism dynamics governed by dose-dependent toxicity of cross-fed nutrients. ISME J. 2016;11:337-48.
18. McCully AL, LaSarre B, McKinlay JB. Recipient-biased competition for an intracellularly generated cross-fed nutrient is required for coexistence of microbial mutualists. mBio. 2017;8:e01620-17.
19. McCully AL, LaSarre B, McKinlay JB. Growth-independent cross-feeding modifies boundaries for coexistence in a bacterial mutualism. Environ Microbiol. 2017;19:3538-50.
20. McCully AL, Behringer MG, Gliessman JR, Pilipenko EV, Mazny JL, Lynch M, et al. An *Escherichia coli* nitrogen starvation response is important for mutualistic coexistence with *Rhodopseudomonas palustris*. Appl Environ Microbiol. 2018;84:e00404-18.
21. Kim M, Zhang Z, Okano H, Yan D, Groisman A, Hwa T. Need-based activation of ammonium uptake in *Escherichia coli*. Mol Syst Biol. 2012;8:616.
22. Walter A, Gutknecht J. Permeability of small nonelectrolytes through lipid bilayer membranes. J Membrane Biol. 1986;90:207-17.
23. Dixon R, Kahn D. Genetic regulation of biological nitrogen fixation. Nat Rev Microbiol. 2004;2:621-31.
24. McKinlay JB, Harwood CS. Carbon dioxide fixation as a central redox cofactor recycling mechanism in bacteria. Proc Natl Acad Sci USA. 2010;107:11669-75.
25. Blattner FR, Plunkett G, Bloch CA, Perna NT, Burland V, Riley M, et al. The complete genome sequence of *Escherichia coli* K-12. Science. 1997;277:1453-62.
26. Kim M-K, Harwood CS. Regulation of benzoate-CoA ligase in *Rhodopseudomonas palustris*. FEMS Microbiol Lett. 1991;83:199-203.
27. Quandt J, Hynes MF. Versatile suicide vectors which allow direct selection for gene replacement in Gram-negative bacteria. Gene. 1993;127:15-21.
28. Datsenko KA, Wanner BL. One-step inactivation of chromosomal genes in *Escherichia coli* K-12 using PCR products. Proc Natl Acad Sci USA. 2000;97:6640-5.
29. Rey FE, Oda Y, Harwood CS. Regulation of uptake hydrogenase and effects of hydrogen utilization on gene expression in *Rhodopseudomonas palustris*. J Bacteriol. 2006;188:6143-52.
30. McKinlay JB, Zeikus JG, Vieille C. Insights into *Actinobacillus succinogenes* fermentative metabolism in a chemically defined growth medium. Appl Environ Microbiol. 2005;71:6651-6.

572 31. Huang JJ, Heiniger EK, McKinlay JB, Harwood CS. Production of hydrogen gas from
573 light and the inorganic electron donor thiosulfate by *Rhodopseudomonas palustris*. Appl Environ
574 Microbiol. 2010;76:7717-22.
575 32. Zhou K, Zhou L, Lim QE, Zou R, Stephanopoulos G, Too H-P. Novel reference genes for
576 quantifying transcriptional responses of *Escherichia coli* to protein overexpression by
577 quantitative PCR. BMC Mol Biol. 2011;12:18.
578 33. Bolger AM, Lohse M, Usadel B. Trimmomatic: a flexible trimmer for Illumina sequence
579 data. Bioinformatics. 2014;30:2114-20.
580 34. Deatherage DE, Barrick JE. Identification of mutations in laboratory-evolved microbes
581 from next-generation sequencing data using breseq. In: Sun L, Shou W, editors. Engineering
582 and analyzing multicellular systems: Methods and protocols. New York, NY: Springer New York;
583 2014. p. 165-88.
584 35. Li H, Durbin R. Fast and accurate short read alignment with Burrows–Wheeler
585 transform. Bioinformatics. 2009;25:1754-60.
586 36. Cingolani P, Platts A, Wang LL, Coon M, Nguyen T, Wang L, et al. A program for
587 annotating and predicting the effects of single nucleotide polymorphisms, SnpEff. Fly.
588 2012;6:80-92.
589 37. Harcombe WR, Chacón JM, Adamowicz EM, Chubiz LM, Marx CJ. Evolution of
590 bidirectional costly mutualism from byproduct consumption. Proc Natl Acad Sci USA.
591 2018;115:12000-4.
592 38. Pande S, Kaftan F, Lang S, Svatoš A, Germerodt S, Kost C. Privatization of cooperative
593 benefits stabilizes mutualistic cross-feeding interactions in spatially structured environments.
594 ISME J. 2015;10:1413-23.
595 39. Lipson DA. The complex relationship between microbial growth rate and yield and its
596 implications for ecosystem processes. Front Microbiol. 2015;6:615.
597 40. Wortel MT, Noor E, Ferris M, Bruggeman FJ, Liebermeister W. Metabolic enzyme cost
598 explains variable trade-offs between microbial growth rate and yield. PLoS Comp Biol.
599 2018;14:e1006010.
600 41. Cheng C, O'Brien EJ, McCloskey D, Utrilla J, Olson C, LaCroix RA, et al. Laboratory
601 evolution reveals a two-dimensional rate-yield tradeoff in microbial metabolism. PLoS Comp
602 Biol. 2019;15:e1007066.
603 42. McDowall JS, Murphy BJ, Haumann M, Palmer T, Armstrong FA, Sargent F. Bacterial
604 formate hydrogenlyase complex. Proc Natl Acad Sci USA. 2014;111:E3948-E56.
605 43. Sangani AA, McCully AL, LaSarre B, McKinlay JB. Fermentative *Escherichia coli* makes
606 a substantial contribution to H_2 production in coculture with phototrophic *Rhodopseudomonas*
607 *palustris*. FEMS Microbiol Lett. 2019;366:fnz162.
608 44. Zimmer DP, Soupene E, Lee HL, Wendisch VF, Khodursky AB, Peter BJ, et al. Nitrogen
609 regulatory protein C-controlled genes of *Escherichia coli*: Scavenging as a defense against
610 nitrogen limitation. Proc Natl Acad Sci USA. 2000;97:14674-9.
611 45. Brown DR, Barton G, Pan Z, Buck M, Wigneshweraraj S. Nitrogen stress response and
612 stringent response are coupled in *Escherichia coli*. Nat Commun. 2014;5:4115.
613 46. Switzer A, Brown DR, Wigneshweraraj S. New insights into the adaptive transcriptional
614 response to nitrogen starvation in *Escherichia coli*. Biochem Soc Trans. 2018:BST20180502.
615 47. Jensen KF. The *Escherichia coli* K-12 "wild types" W3110 and MG1655 have an rph
616 frameshift mutation that leads to pyrimidine starvation due to low pyrE expression levels. J
617 Bacteriol. 1993;175:3401-7.
618 48. LaCroix RA, Sandberg TE, O'Brien EJ, Utrilla J, Ebrahim A, Guzman GI, et al. Use of
619 adaptive laboratory evolution to discover key mutations enabling rapid growth of *Escherichia coli*
620 K-12 MG1655 on glucose minimal medium. Appl Environ Microbiol. 2015;81:17-30.
621 49. Ko M, Park C. H-NS-dependent regulation of flagellar synthesis is mediated by a LysR
622 family protein. J Bacteriol. 2000;182:4670-2.

623 50. Krin E, Danchin A, Soutourina O. Decrypting the H-NS-dependent regulatory cascade of
624 acid stress resistance in *Escherichia coli*. BMC Microbiol. 2010;10:273.
625 51. Weglenski P, Ninfa AJ, Ueno-Nishio S, Magasanik B. Mutations in the *glnG* gene of
626 *Escherichia coli* that result in increased activity of nitrogen regulator I. J Bacteriol.
627 1989;171:4479-85.
628 52. Dixon R, Eydmann T, Henderson N, Austin S. Substitutions at a single amino acid
629 residue in the nitrogen-regulated activator protein NTRC differentially influence its activity in
630 response to phosphorylation. Mol Microbiol. 1991;5:1657-67.
631 53. Hart SFM, Pineda JMB, Chen C-C, Green R, Shou W. Disentangling strictly self-serving
632 mutations from win-win mutations in a mutualistic microbial community. bioRxiv. 2019:530287.
633 54. Waite AJ, Shou W. Adaptation to a new environment allows cooperators to purge
634 cheaters stochastically. Proc Natl Acad Sci USA. 2012;109:19079-86.
635 55. Estrela S, Morris JJ, Kerr B. Private benefits and metabolic conflicts shape the
636 emergence of microbial interdependencies. Environ Microbiol. 2016;18:1415-27.
637 56. Warsi OM, Andersson DI, Dykhuizen DE. Different adaptive strategies in E. coli
638 populations evolving under macronutrient limitation and metal ion limitation. BMC Evol Biol.
639 2018;18:72.
640 57. Rosenzweig RF, Sharp RR, Treves DS, Adams J. Microbial evolution in a simple
641 unstructured environment: genetic differentiation in *Escherichia coli*. Genetics. 1994;137:903-
642 17.
643 58. Treves DS, Manning S, Adams J. Repeated evolution of an acetate-crossfeeding
644 polymorphism in long-term populations of *Escherichia coli*. Mol Biol Evol. 1998;15:789-97.
645 59. Larimer FW, Chain P, Hauser L, Lamerdin J, Malfatti S, Do L, et al. Complete genome
646 sequence of the metabolically versatile photosynthetic bacterium *Rhodopseudomonas palustris*.
647 Nat Biotechnol. 2004;22:55-61.
648 60. Hayashi K, Morooka N, Yamamoto Y, Fujita K, Isono K, Choi S, et al. Highly accurate
649 genome sequences of *Escherichia coli* K-12 strains MG1655 and W3110. Mol Syst Biol.
650 2006;2:2006.0007.
651 61. Simon R, Priefer U, Pühler A. A broad host range mobilization system for in vivo genetic
652 engineering: transposon mutagenesis in Gram negative bacteria. Biotechnol. 1983;1:784-91.

FIGURE LEGENDS

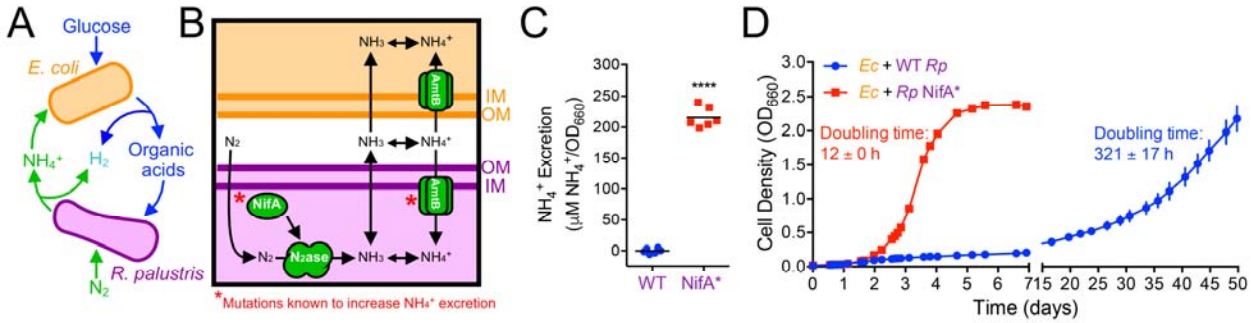

Fig. 1. Mutualistic cross-feeding between *E. coli* and *R. palustris* is facilitated by NH_4^+ excretion. (A) Coculture growth requires reciprocal cross-feeding of organic acids and NH_4^+ excreted by *E. coli* and *R. palustris*, respectively. (B) Mechanism of NH_4^+ cross-feeding from *R. palustris* to *E. coli* and mutational targets known to increase NH_4^+ excretion by *R. palustris* (*). (C) NH_4^+ excretion levels by WT *R. palustris* (CGA009) and an isogenic NifA* mutant (CGA676) in carbon-limited N_2-fixing monocultures grown in grown in MDC or NFM minimal medium, with similar results observed for both media. Points are biological replicates and lines are means, n=6; paired t-test, ****p<0.0001. (D) Coculture growth curves (both species) of *E. coli* paired with either WT *R. palustris* or the NifA* mutant. Points are means ± SEM, n=3. Doubling times are means ± SD.

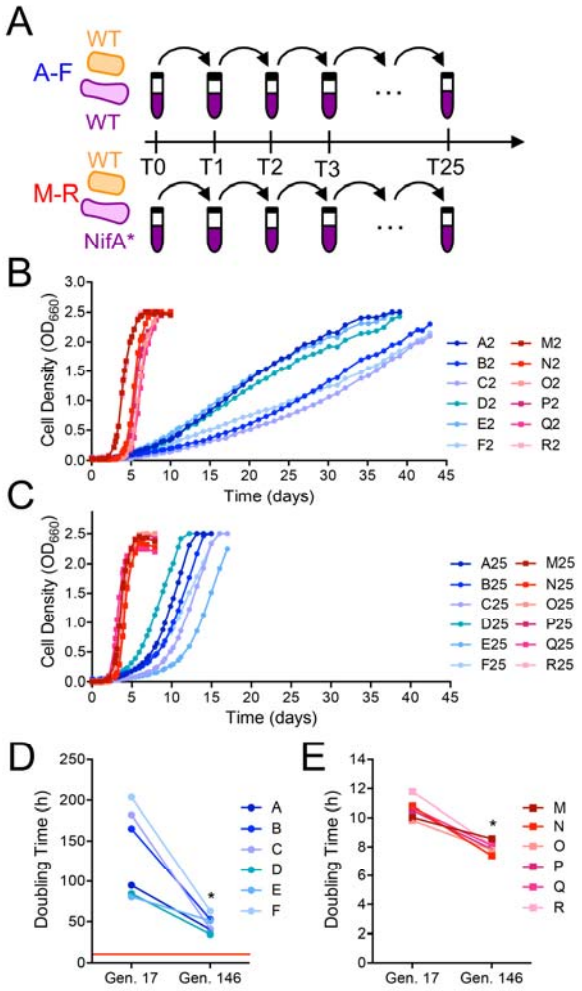

Fig. 2. Coculture doubling times decreased during experimental evolution of WT-based (CGA4001; blue) and NifA*-based (CGA4003; red) cocultures. Points are values for the indicated individual revived coculture lineages. (A) Design for experimental evolution of parallel WT-based (A-F) and NifA*-based (M-R) cocultures via serial transfer. (B, C) Growth curves (both species) of WT-based (blue circles) and NifA*-based (red squares) cocultures revived after two transfers (17 generations) (B) or 25 transfers (146 generations) (C) of experimental evolution. Different shades indicate the different lineages. (D, E) Coculture doubling times (both species) of individual WT-based cocultures (D) or NifA* based cocultures (E) at generation (Gen.) 17 and 146 (*, Wilcoxon matched-pairs signed rank, p=0.0313). (D) The red line indicates the doubling time of NifA*-based cocultures at Gen. 17.

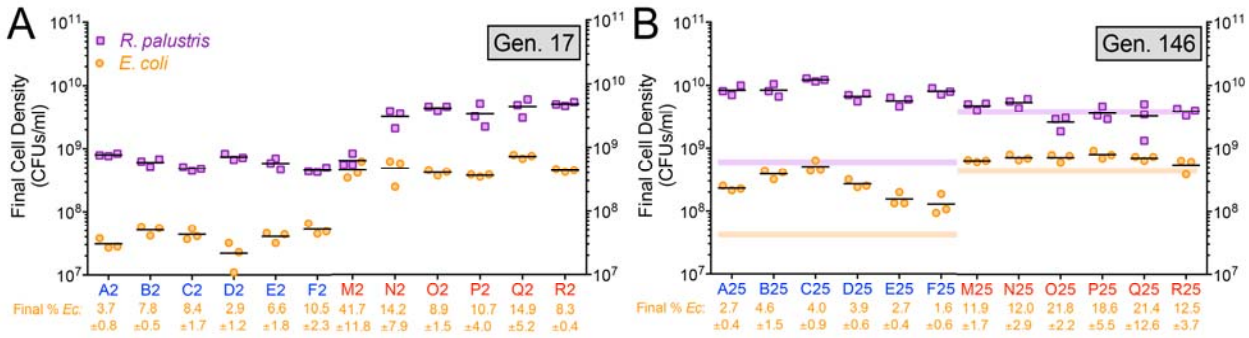

Fig. 3. Final cell densities for each species increase in WT-based cocultures between generation 17 (A) and generation 146 (B). (A, B) Final viable cell densities (colony forming units [CFUs/ml]) of *R. palustris* and *E. coli* and the final *E. coli* percentage (± SD) for WT-based (CGA4001; blue) and NifA*-based (CGA4003; red) cocultures at the final time points shown in Fig 2B and 2C. Points represent technical replicates of CFUs/ml for each lineage and lines are means, n=3. The purple and orange lines in panel B indicate the median CFUs/ml for *R. palustris* and *E. coli*, respectively, at generation 17 for reference. The lower *R. palustris* CFUs in the M2 coculture was due to plate contamination that obscured accurate CFU enumeration. The average final *E. coli* percentage did not differ significantly between WT-based and NifA*-based cocultures at Gen. 17 whether we included or excluded M2 values (Wilcoxon matched-pairs signed rank test, P=0.563 or 0.125).

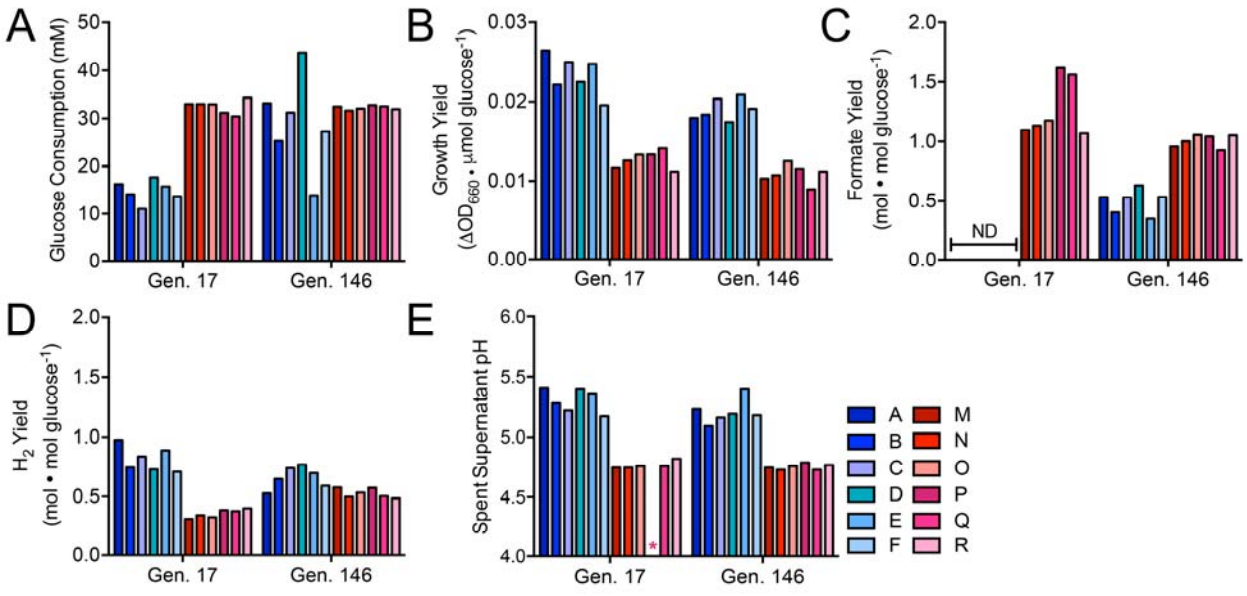

689

690 **Fig. 4.** WT-based (blue) and NifA*-based (red) cocultures exhibit distinct metabolic phenotypes.
691 Bars represent a single measurement for each lineage for glucose consumption (A), growth
692 yield (B), formate yield (C), H_2 yield (D), and final pH (E) for the indicated WT-based (CGA4001;
693 blue) and NifA*-based (CGA4003; red) revived coculture lineages at generation (Gen) 17 and
694 146. Different shades indicate different lineages. ND, not detected. Asterisk (*) indicates that the
695 pH for lineage P at G17 was not quantified because culture tube broke prior to measurement.

696

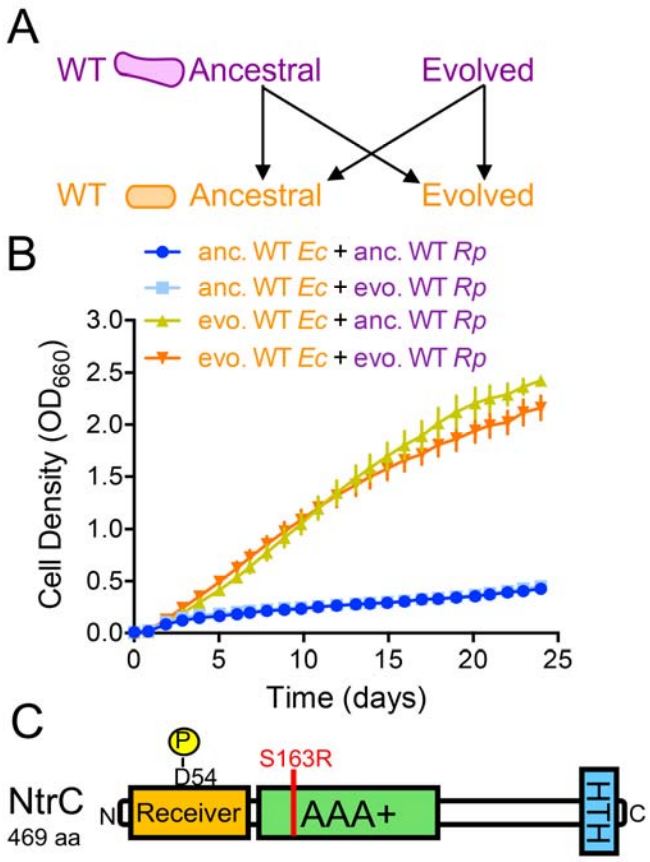

Fig. 5. Adaptation by *E. coli* is sufficient to enable growth of WT-based cocultures. Ancestral (anc) and evolved (evo) WT *R. palustris* (CGA4001) and WT *E. coli* were paired in all possible combinations (A) and the growth of the cocultures (both species) was monitored (B). (B) Points are means ± SEM, n=3. (C) The location (red line) of the missense mutation in *E. coli* NtrC, which was fixed in all six parallel evolved *E. coli* populations from WT-based cocultures at G140-146.

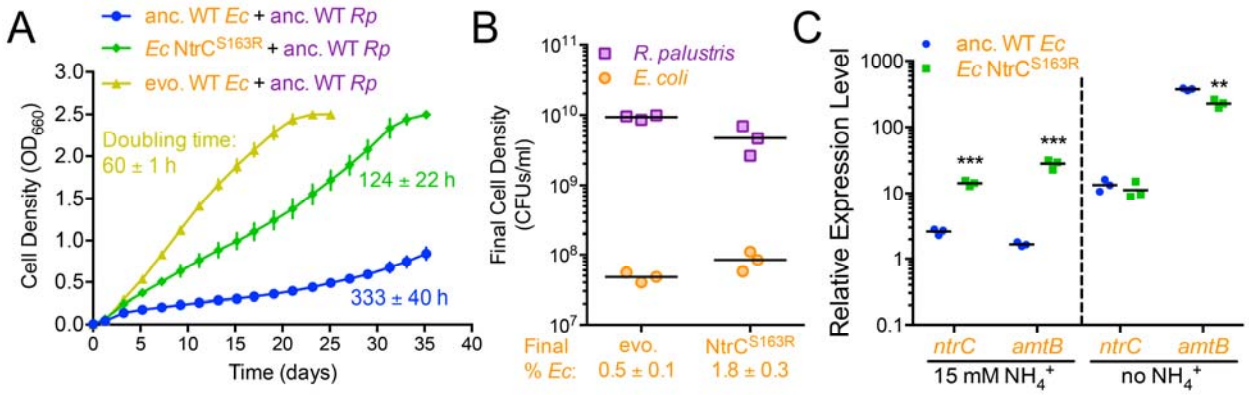

705

706 **Fig. 6.** A missense mutation in *E. coli ntrC* enables emergent NH_4^+ cross-feeding by conferring
707 constitutive expression of nitrogen acquisition. (A) Coculture growth curves (both species) of
708 ancestral (anc) WT, evolved (evo) WT, and the $NtrC^{S163}$ mutant *E. coli* paired with ancestral WT
709 *R. palustris* (CGA4001). Points are means ± SEM, n=3. Mean doubling times (± SD) are listed
710 next to each growth curve. (B) Final cell densities of each species and *E. coli* frequencies in
711 cocultures with evolved WT *E. coli* and the $NtrC^{S163}$ mutant at the final time points shown in
712 panel A. Triplicate technical replicate plating was performed for each biological replicate. Final
713 *E. coli* frequencies are the mean ± SD. (C) Relative expression of *ntrC* and *amtB* genes in
714 ancestral WT *E. coli* and the $NtrC^{S163}$ mutant when grown in monoculture with 15 mM NH_4Cl or
715 under complete NH_4Cl starvation. (B, C) Points represent biological replicates and lines are
716 means, n=3; Holm-Sidak t-test, $^{**}p<0.01$, $^{***}p<0.001$). RT-qPCR experiments were performed
717 with duplicate technical replicates for each biological replicate. *E. coli hcaT* was used for
718 normalization. Similar results were observed with *gyrB* and with multiple primer sets for both the
719 target and reference housekeeping genes.

720 **Table 1. Parallel mutations in evolved WT-based and NifA*-based cocultures**
721

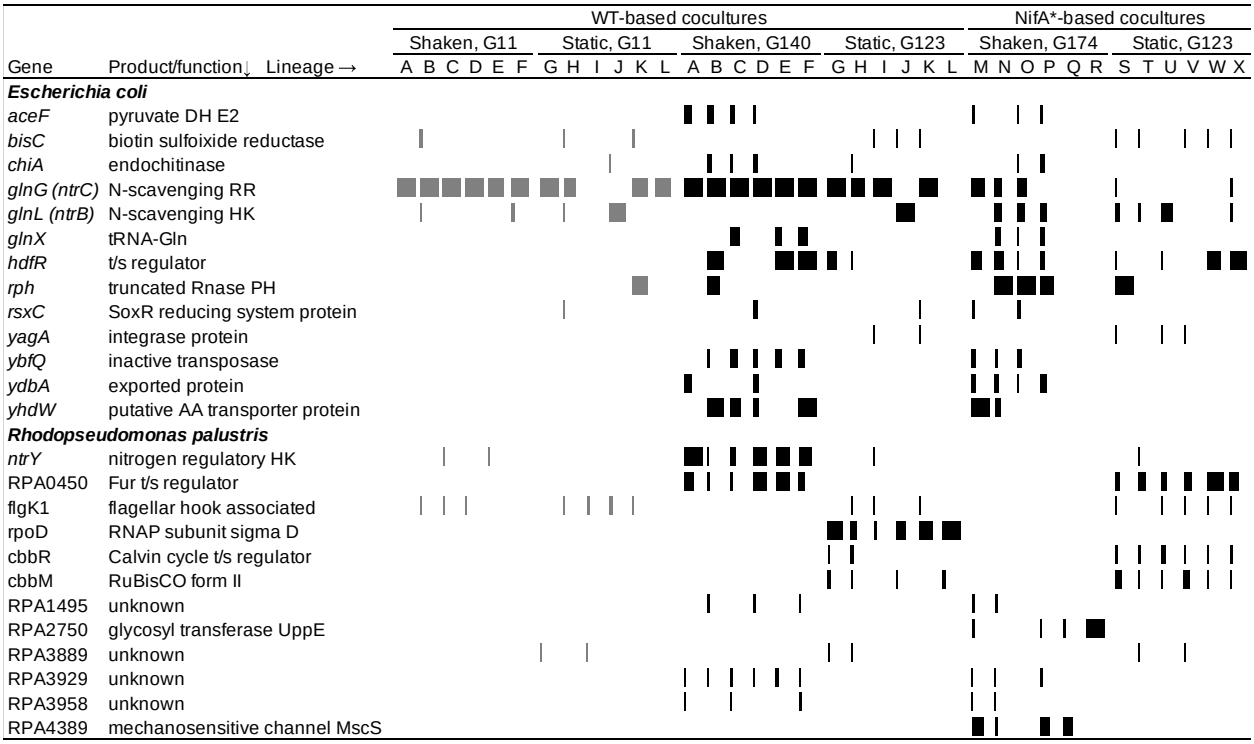

722
723

724 Genes included have > 1 missense mutation, premature stop, insertion, and/or deletion in > 4
725 lineages, have passing scores, and occur at frequency of > 5% within a population at the later
726 time point (black bars). Bar width corresponds to mutation frequency. Frequencies at the early
727 time point for the genes with the above criteria are also shown (gray bars). The highest
728 frequency was used when multiple mutations were identified in a single gene within a single
729 lineage. Coverage was too low to detect mutations in E. coli lineages Q and R. Details of these
730 and other mutations, including intergenic mutations with high parallelism that were omitted here
731 for simplicity, are in Supplementary Files 1 and 2. DH, dehydrogenase; HK, histidine kinase;
732 RR, response regulator; t/s transcription.

SUPPLEMENTARY INFORMATION

Enhanced nutrient uptake is sufficient to drive emergent cross-feeding between bacteria in a synthetic community

Running title. Cross-feeding driven by enhanced nutrient uptake.

Ryan K Fritts[1], Jordan T Bird[2], Megan G Behringer[3], Anna Lipzen[4], Joel Martin[4], Michael Lynch[3], and James B McKinlay[1]*

[1]Department of Biology, Indiana University Bloomington, Bloomington, IN, 47405

[2]Department of Biochemistry and Molecular Biology, University of Arkansas for Medical Sciences, Little Rock, AR, 72205

[3]School of Life Sciences, Biodesign Center for Mechanisms of Evolution, Arizona State University, Tempe, AZ, 85281

[4]Department of Energy Joint Genome Institute, Walnut Creek, CA, 94598

*Corresponding author

1001 E 3rd St, Jordan Hall, Bloomington, IN 47405

Phone: 812-855-0359

Email: jmckinla@indiana.edu

Supplemental File 1. Mutations identified in evolved WT-based cocultures A25, B24-F24 and NifA*-based cocultures M30-R30 using *breseq*.

Supplemental File 2. Mutations identified in evolved WT-based cocultures A1-F1 (mixed/shaking), G1-L1 (static), G21-L21 (static), and NifA*-based cocultures S21-X21 (static) using the BBMap package

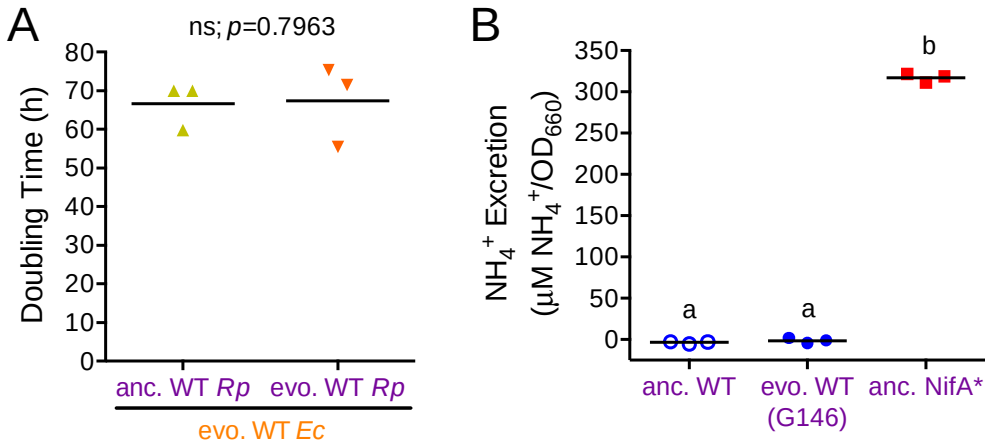

Fig. S1. Evolution of WT *R. palustris* in coculture with *E. coli* does not affect coculture doubling times nor NH_4^+ excretion levels. (A) Coculture doubling time of evolved WT *E. coli* (G146, A25 isolates) paired with ancestral or evolved WT *R. palustris* (CGA4001; G146, A25 isolates). Points represent biological replicates and lines are means, n=3; paired t-test, *p*=0.7963; ns, not significant). (B) NH_4^+ excretion by ancestral and evolved WT *R. palustris* and the NifA* mutant during carbon-limited N_2-fixing monoculture growth. Points represent biological replicates and lines are means, n=3; One-way ANOVA with Tukey's multiple comparisons test, different letters indicate significant statistical differences, p<0.0001).

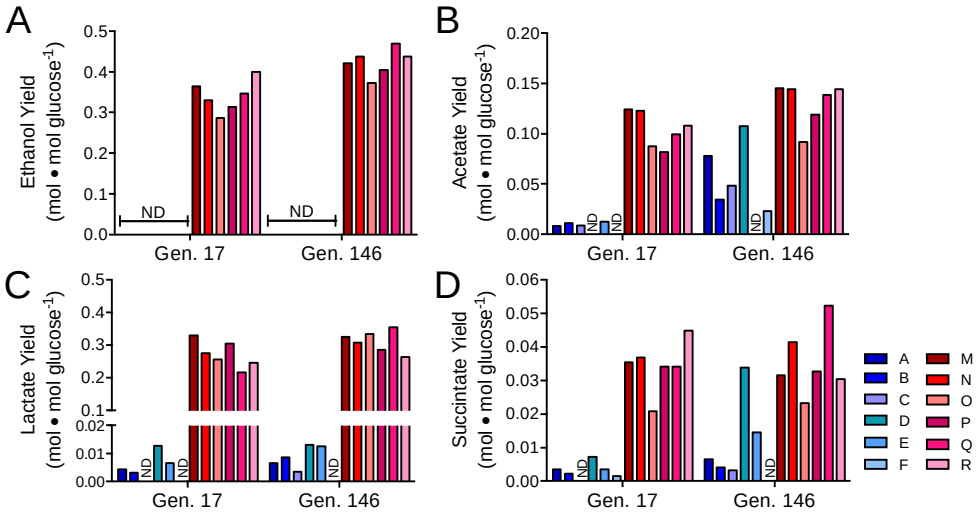

Fig. S2. Other evolved coculture fermentation product yields also differ between WT-based and NifA*-based cocultures. Bars are individual yields for ethanol (A), acetate (B), lactate (C), and succinate (D), for the indicated WT-based (CGA4001; blue) and NifA*-based (CGA4003; red) revived coculture lineages at generation (Gen) 11 and 146. Different shades indicate different lineages. ND, not detected.

800 **Supplementary Table S1. Strains and plasmids.**
801

Strain or plasmid	Genotype (text designation); Phenotype/description	Reference, origin, or description
R. palustris strains		
CGA009	Wild-type strain; spontaneous Cm^R derivative of CGA001	[59]
CGA676	NifA* (NifA*); derivative of CGA009 with 48 bp deletion of NifA Q-linker (amino acids 202-217) conferring constitutive nitrogenase expression	[24]
CGA4001	Δ*hupS* (anc. WT); Ancestral strain for experimentally evolved WT-based cocultures A-F; derivative of CGA009 with inactive uptake hydrogenase	This study
CGA4003	*nifA** Δ*hupS* (anc. NifA*); Ancestral strain for experimentally evolved NifA*-based cocultures M-R; derivative of CGA009 with constitutive nitrogenase expression and inactive uptake hydrogenase	This study
E. coli strains		
MG1655	Wild-type K-12 strain (WT/anc.); ancestral *E. coli* strain for all experimental evolution lineages	[60]
MG1655 $NtrC^{S163R}$	$NtrC^{S163R}$ ($NtrC^{S163R}$); MG1655 derivative with serine 163 to arginine (S163R) point mutation of NtrC	This study
S17-1	*thi pro hdsR hdsM*$^+$ *recA*; chromosomal insertion of RP4-2 (Tc::Mu Km::Tn7);	[61]
Plasmids		
pJQ200SK		[27]
pJQ-ΔhupS	pJQ200SK with DNA fragments flanking *hupS* fused by PCR to generate unmarked, in-frame deletion of *hupS* in *R. palustris*	[17]
pKD46	Cb^R; temperature-sensitive plasmid with arabinose-inducible λ-Red recombination system for recombineering of *E. coli*	[28]

802

803 **Supplementary Table S2. Primers**

Primer	Sequence (5'→3'); Restriction site	Purpose
Cloning primers		
sacB-Gm^R Fwd	CAGCAATTTGCGCTCAATAATCAATCTTTACACACAAGCT GTGAAGCTAGAGGATCGATCCTTTTTAACC	Amplifying *sacB*-GmR from pJQ200SK with 45 bp *ntrC* upstream flanking region
sacB-Gm^R Rev	CGAGTTCTCGGTTTACCTGCCTATCAGGAAATAAAGGTG ACGTTTGAAACGGATGAAGGCACGAAC	Amplifying *sacB*-GmR from pJQ200SK with 45 bp *ntrC* downstream flanking region
ntrC us R2	CATACTGAACTTATCGGAACAGTAAAGCGTAAAATACCA GCAATTTGCGCTCAATAATC	Adding additional 35 bp of *ntrC* upstream flanking region to sacB-GmR product in 2nd round of PCR for λ-Red recombineering
ntrC ds R2	CAGGCAAAATTGAATTTACCAGTTGGCCAGGGCATACCG AGTTCTCGGTTTACCTGC	Adding additional 35 bp of ntrC downstream flanking region to sacB-GmR product in 2nd round of PCR for λ-Red recombineering
ntrC Fwd	GCGCGGATTGATGTGGAAG	Amplfying *E. coli* ntrC with >200 bp upstream stream flanking region from evolved *E. coli* for λ-Red recombineering
ntrC Rev	CAGCTAAACAGCCCAATCATTG	Amplfying *E. coli* ntrC with ~200 bp downstream flanking region from evolved *E. coli* for λ-Red recombineering
ALP011	TGGATCCGCGACACCTCGCTGTCG	Amplifying *R. palustris hupS* upstream flanking region for in-frame deletion; BamHI
ALP012	CCGTTGGAGGTGCCGGGTACCCTCGTAAAAGGTTTCCG TCACTGC	Amplifying *R. palustris hupS* upstream flanking region for in-frame deletion
ALP013	GAAACCTTTTACGAGGGTACCCGGCACCTCCAACGGCA AGTCGGC	Amplifying *R. palustris hupS* downstream flanking region
ALP014	TTCTAGAACCCGGCAATCGCCACC	Amplifying *R. palustris hupS* downstream flanking region; XbaI

qPCR primers		
qPCR *amtB* Fwd1	GGATGATCCCTGCGATGTCTT	Quantifying *E. coli amtB* expression from cDNA; set 1
qPCR *amtB* Rev1	CGAGCTGGCGGCAAAAATC	Quantifying *E. coli amtB* expression from cDNA; set 1
qPCR *amtB* Fwd2	GCGGTGATGGGCAGCATTTATC	Quantifying *E. coli amtB* expression from cDNA; set 2
qPCR amtB Rev2	AGCGCCCCAACTATCAAGC	Quantifying *E. coli amtB* expression from cDNA; set 2
qPCR *ntrC* Fwd1	GGAATAATGTACCGCCATCGGC	Quantifying *E. coli ntrC* expression from cDNA; set 1
qPCR *ntrC* Rev1	ATCAGAACTGTTTGGCCACGAG	Quantifying *E. coli ntrC* expression from cDNA; set 1
qPCR *ntrC* Fwd2	ACTCTCCGCAACCGTTGATTC	Quantifying *E. coli ntrC* expression from cDNA; set 2
qPCR NtrC Rev2	AGCTGGAAAACACCTGCCG	Quantifying *E. coli ntrC* expression from cDNA; set 2
qPCR hcaT Fwd	CGTGGTGGCGGAAGTCATTATC	Quantifying *E. coli hcaT* expression from cDNA; housekeeping reference gene
qPCR hcaT Rev	CGCCGAGATCAACAGCATATCG	Quantifying *E. coli hcaT* expression from cDNA; housekeeping reference gene
qPCR gyrB Fwd	CGTAGATCTGACGGTGAATTT	Quantifying *E. coli gyrB* expression from cDNA; housekeeping reference gene
qPCR gyrB Rev	CGTTGGTGTTTCGGTAGTA	Quantifying *E. coli gyrB* expression from cDNA; housekeeping reference gene

804
805

Supplementary Table 3. Mutations in *ntrBC* genes in *E. coli* following coculture evolution

Lineage	Gene	Mutation	Generation	Frequency	*R. palustris* partner strain	Growth condition	SRA Accession
A	*ntrC*	S163R	11	100%	WT	Mixed	SRX5772396
A	*ntrC*	S163R	146	100%	WT	Mixed	SRX5872514
B	*ntrC*	S163R	11	NC[a]	WT	Mixed	SRX5772395
B	*ntrC*	S163R	140	100%	WT	Mixed	SRX5872520
C	*ntrC*	S163R	11	NC[a]	WT	Mixed	SRX5772261
C	*ntrC*	S163R	140	100%	WT	Mixed	SRX5874533
D	*ntrC*	S163R	11	NC[a]	WT	Mixed	SRX5772258
D	*ntrC*	S163R	140	100%	WT	Mixed	SRX5874537
E	*ntrC*	S163R	11	NC[a]	WT	Mixed	SRX5772266
E	*ntrC*	S163R	140	100%	WT	Mixed	SRX5874556
F	*ntrC*	S163R	11	NC[a]	WT	Mixed	SRX5209606
F	*ntrC*	S163R	140	100%	WT	Mixed	SRX5874560
G	*ntrC*	S163R	11	NC[a]	WT	Static	SRX5772260
G	*ntrC*	P399T	11	17%	WT	Static	SRX5772260
G	*ntrC*	S163R	123	100%	WT	Static	SRX5772001
H	*ntrC*	S163R	11	63%	WT	Static	SRX5772264
H	*ntrC*	S163R	123	76%	WT	Static	SRX5771991
I	*ntrC*	S163R	11	NC[a]	WT	Static	SRX5772259
I	*ntrC*	S163R	123	100%	WT	Static	SRX5771995
J	*ntrB*	R116S	11	NC[a]	WT	Static	SRX5772262
J	*ntrB*	R116S	123	100%	WT	Static	SRX5771992
K	*ntrC*	S163R	11	80%	WT	Static	SRX5772263
K	*ntrC*	S163R	123	100%	WT	Static	SRX5771996
L	*ntrC*	S163	11	NC[a]	WT	Static	SRX5772265
L	ND[b]	-	123	-	WT	Static	SRX5209608
M	*ntrC*	H184Y	174	79%	NifA*	Mixed	SRX5874674
N	*ntrB*	A175V	174	39%	NifA*	Mixed	SRX5875647
N	*ntrC*	D109V	174	10%	NifA*	Mixed	SRX5875647
N	*ntrC*	G373V	174	44%	NifA*	Mixed	SRX5875647
O	*ntrB*	P336Q	174	41%	NifA*	Mixed	SRX5877494
O	*ntrC*	Q374H	174	54%	NifA*	Mixed	SRX5877494
P	*ntrB*	R116H	174	32%	NifA*	Mixed	SRX5877497
Q	ND[b]	-	174	-	NifA*	Mixed	SRX5910505
R	ND[b]	-	174	-	NifA*	Mixed	SRX5910551
S	*ntrB*	L137V	123	23%	NifA*	Static	SRX5771990
S	*ntrC*	S45R	123	7%	NifA*	Static	SRX5771990
T	*ntrB*	G150C	123	15%	NifA*	Static	SRX5771989
U	*ntrB*	A175V	123	65%	NifA*	Static	SRX5771988
V	ND[b]	-	-	-	NifA*	Static	SRX5771994
W	ND[b]	-	-	-	NifA*	Static	SRX5771993
X	*ntrB*	A175V	123	13%	NifA*	Static	SRX5771967
X	*ntrB*	V305F	123	16%	NifA*	Static	SRX5771967
X	*ntrC*	E116K	123	17%	NifA*	Static	SRX5771967

[a]Frequency was not calculated (NC) because read coverage <10.

[b]*ntrBC* mutations were not detected (ND) in population. Mutations present at frequencies <1% are not listed.